

Mineralogical characterization of some V-type asteroids, in support of the NASA *Dawn* mission[★]

Maria Cristina De Sanctis,^{1†} Eleonora Ammannito,² Alessandra Migliorini,¹
Daniela Lazzaro,³ Maria Teresa Capria¹ and Lucy McFadden⁴

¹*Istituto di Astrofisica Spaziale e Fisica Cosmica, Area di Ricerca Tor Vergata, via del Fosso del Cavaliere 100, 00133 Roma, Italy*

²*Istituto di Fisica dello Spazio Interplanetario, Area di Ricerca Tor Vergata, via del Fosso del Cavaliere 100, 00133 Roma, Italy*

³*Observatório Nacional, Rua Gal. José Cristino 77, Rio de Janeiro, 20921-400 RJ, Brazil*

⁴*Goddard Space Flight Center, Greenbelt, MD 20771, USA*

Accepted 2010 November 22. Received 2010 October 22; in original form 2010 April 29

ABSTRACT

We present new reflectance spectra of 12 V-type asteroids obtained at the 3.6 m Telescopio Nazionale Galileo (TNG) covering the spectral range 0.7 to 2.5 μm . This spectral range, encompassing the 1 and 2 μm , pyroxene features, allows a precise mineralogical characterization of the asteroids. The spectra of these asteroids are examined and compared to spectra for the Howardite, Eucrite and Diogenite (HED) meteorites, of which Vesta is believed to be the parent body. The observed objects were selected from different dynamical populations with the aim to verify if there exist spectral parameters that can shed light on the origin of the objects. A reassessment of data previously published has also been performed using a new methodology. We derive spectral parameters from NIR spectra to infer mineralogical information of the observed asteroids.

The V-type asteroids here discussed show mainly orthopyroxene mineralogy although some of them seem to have a mineralogical composition containing cations that are smaller than Mg cations. Most of the observed Vestoids show a low abundance of Ca (<10 per cent Wo). This result implies that no one of the Vestoids studied consists of just eucritic material, but they must additionally have a diogenitic component. However, we must remember that the ground-based data are subject to larger errors than the laboratory data used as reference spectra for interpretation.

Finally, we note that the intermediate belt asteroid (21238) 1995WV7 has spectral parameters quite different from the observed V-type objects of the inner belt, so it could be a basaltic asteroid not related to Vesta.

This mineralogical analysis of asteroids related to Vesta is done in support of NASA's *Dawn* mission, which will enter into orbit around Vesta in the summer of 2011. This work extends the scientific context of the mission to include processes contributing to the nature of smaller V-type asteroids that may be related to Vesta.

Key words: minor planets, asteroids general – minor planets, asteroids: individual: 4 Vesta.

1 INTRODUCTION

Asteroid (4) Vesta is the only known large asteroid with a basaltic crust that was first inferred by McCord, Adams & Johnson (1970) from visible spectra. Subsequent works (McFadden, McCord &

Pieters 1977; Larson & Fink 1975; Gaffey 1997; Binzel et al. 1997) proved that this was indeed the case. To have this composition, the asteroid must have undergone extensive differentiation and resurfacing, being possibly the smallest differentiated object in the Solar system. For this reason, it is the target of the *Dawn* mission that will arrive at (4) Vesta in 2011. *Dawn* will remain in orbit around Vesta for several months (Russell et al. 2004, 2007).

The composition of (4) Vesta is similar to that of the basaltic achondrite meteorites, in particular the HED suite that encompasses the eucrites, the diogenites and the howardites (see Section 5 for a more detailed description). These achondrite meteorites include

[★]Based on observations made with the Italian Telescopio Nazionale Galileo (TNG) operated on the island of La Palma by the Centro Galileo Galilei of the INAF (Istituto Nazionale di Astrofisica) at the Spanish Observatorio de Roque de los Muchachos of the Instituto de Astrofísica de Canarias.

[†]E-mail: mariacristina.desanctis@iasf-roma.inaf.it

magmatic rocks formed at high temperature. They are all thought to come from a large asteroid, which melted to form a metallic core and basaltic magmas, after its formation. A close connection between asteroid (4) Vesta and these basaltic achondrites was established during the latest studies, which include dynamical simulations, infrared reflectance spectroscopic investigation and *Hubble Space Telescope (HST)* observations.

Although (4) Vesta is the only large object in the Main Belt which shows basaltic crust, an increasingly large number of small asteroids with a similar surface have been discovered (V-type asteroids), posing the possibility of the presence of additional differentiated bodies in the asteroid belt. HED meteorites do not come directly from (4) Vesta, but they possibly come from smaller asteroids that are spectrally similar to Vesta and could be collisionally derived pieces of Vesta. Some of these objects are linked to Vesta, belonging to the Vesta family, while others do not have a clear dynamical link with Vesta, suggesting the presence of other basaltic parent bodies. A strong indication of the presence of multiple basaltic asteroids, at least in the early phases of our Solar system, and hence the existence of more than one source where HEDs meteorites can come from, arises from diverse studies of the HED meteorites. The first indication came from NWA 011, a meteorite mineralogical similar to the basaltic eucrites but having very different oxygen isotopic and pyroxene composition, indicating that it probably originated from a body distinct from that of most HEDs (Yamaguchi et al. 2002; Floss et al. 2005). Very precise oxygen isotopic composition measurements have indicated that although most HEDs are from the same parent body, four to six of them have values which are incompatible with a single origin for all HEDs (Greenwood et al. 2005; Scott et al. 2009).

The discovery of small basaltic asteroids in the outer (Lazzaro et al. 2000) and intermediate (Binzel, Masi & Foglia 2006; Hammergren, Gyuk & Puckett 2006) Main Belt, as well as in the inner belt but far away from the dynamical limits of the Vesta family (Xu et al. 1995; Burbine, Buchanan & Binzel 2001; Duffard et al. 2004; Alvarez-Candal et al. 2006), seems to reinforce the hypothesis that several differentiated parent bodies could have formed. In addition, searches for meteorites in Antarctica resulting in new types of differentiated meteorites such as GRA 06128 and 06129 (Arai et al. 2008) suggest that multiple differentiated planetesimals existed in the early Solar system.

Here, we examine the basaltic material in the main belt to see if there are distinct spectral characteristics that enable distinction between Vesta and non-Vesta family objects, indicative of different origins. Duffard et al. (2004) made a first attempt: the mineralogical analysis of two groups of basaltic asteroids belonging to Vesta's family and in the neighbourhood of Vesta showed the possible presence of distinct mineralogies. However, their results are not conclusive. According to Florczak, Lazzaro & Duffard (2002), V-type asteroids not members of the Vesta family have spectra with a 1 μm band deeper than the family members and Vesta itself. This characteristic would imply that two distinct mineralogical groups, either probing different layers of Vesta (Marzari et al. 1996) or coming from different bodies, would coexist, as already suggested by Vilas, Cochran & Jarvis (2000). The recent work by Moskovitz et al. (2010), on the other hand, found that amongst the inner Main Belt asteroids there is no evidence for non-Vestoid mineralogies. Instead, according to their analysis, these asteroids seem to represent a continuum of compositions, consistent with an origin from a single differentiated parent body.

Considering all the open questions discussed above we believe that only a better mineralogical characterization of all the different

classes of V-type asteroids can shed light on their unique or distinct origin and their relations with HEDs.

It is important to stress that most of the asteroids discussed above have been observed only in the visible wavelength, some of them, up to 1.6 μm , and very few to 2.5 μm . However, only observations up to 2.5 μm , which encompass the second pyroxene band, allow a precise mineralogical characterization (Cloutis et al. 1986; Gaffey et al. 1993, 2002). Therefore, we began a systematic mineralogical study of diverse V-type asteroids, starting with those in the neighbourhood of Vesta (Duffard et al. 2004) and recently including V-type asteroids located far from Vesta. Here, we will discuss the new results obtained after observations at Telescopio Nazionale Galileo (TNG), in La Palma Island, and we will compare them to those obtained in the previous observing run. Moreover, we will make a comparison with spectral and mineralogical parameters of HED meteorites and (4)Vesta.

This study aims to infer the mineralogical composition of the observed Vestoids in order to better understand their link with (4) Vesta and HEDs. The combined indications for mechanisms ejecting material from the Vesta's surface, and dynamical path by which to deliver this material to Earth, have led to believe that Vesta is the parent body for the HED family. This relationship allows us to link geochemical data collected on the HED meteorites to the surface measurements taken by *Dawn*. We think that if the observed Vestoids are originated from Vesta, the spectral variability observed among them should be found also on Vesta's surface. In this case, a more deep understanding of their characteristic spectra will help in the interpretation of the data of the Visible and Infrared Mapping Spectrometer (VIR-MS) onboard the *Dawn* mission spacecraft when it will observe the surface of Vesta (De Sanctis et al. 2010). This instrument will analyse the surface of Vesta producing surface spectral maps. The comparisons between spectral parameters of HEDs, Vesta and individual Vestoids should allow us to better constrain the link between Vesta-Vestoids-HEDs. Understanding the relation between the spectral and petrologic variety of the HEDs Vestoids may allow us to distinguish different igneous provinces on Vesta's surface, thereby using the HEDs as a spectral ground truth for the data return from *Dawn*.

2 OBSERVATIONS AND DATA REDUCTION

Twelve asteroids were selected from a data set of already known V-type asteroids, seven of them being members of the Vesta family, according to Mothé-Diniz, Roig & Carvano (2005). The dynamical classification of the observed asteroids as Vesta family or non-Vesta family is indicated in Table 1. The proper orbital parameters, taken from astdys web site (<http://hamilton.dm.unipi.it/astdys/>), the absolute magnitude and the diameter, obtained assuming an albedo of 0.42, similar to that of (4) Vesta, are provided in Table 1.

We acquired near-infrared (NIR) spectra of the selected asteroids with the TNG, a 3.6 m class telescope in La Palma, during a two-night program, on 2007 December 25–26. We used the Near-Infrared Camera Spectrometer (NICS) equipped with the Amici grism, and a 1-arcsec slit, for the first night and a 0.5-arcsec slit during the second night. NICS offers a unique, high throughput, low-resolution spectroscopic mode with an Amici grism disperser, which yields a complete 0.8–2.5 μm spectrum in one single acquisition. The low resolution together with the high efficiency of the Amici grism (90 per cent in all the infrared range) allowed us to obtain spectra of faint objects like small V-type asteroids with the advantage of having the whole NIR range measured simultaneously. The identification of the objects was done by taking images through

Table 1. Orbital parameters, absolute magnitude, diameter and dynamical classification for each observed asteroid. The orbital parameters are taken from astdys web site (<http://hamilton.dm.unipi.it/astdys/>) and the diameters are computed assuming an albedo of 0.42 (as Vesta) (Tedesco 1989).

Asteroid	<i>a</i> (au)	<i>e</i>	<i>i</i> (°)	<i>H</i>	Diameter (km)	Vesta family
1929 Kollaa	2.363	0.114	7.065	12.52	7.5	Yes
1933 Tinchén	2.353	0.094	9.468	12.92	5.5	Yes
2011 Veteraniya	2.387	0.111	6.367	12.83	5.5	Yes
2912 Lapalma	2.289	0.117	6.742	12.51	6.0	No
3944 Halliday	2.368	0.109	6.754	13.02	5.0	Yes
3968 Koptelov	2.321	0.091	6.679	12.83	5.5	Yes
4147 Lennon	2.362	0.102	6.482	12.87	5.2	Yes
4993 Cossard	2.369	0.091	6.373	13.13	5.2	Yes
6406 1992 MJ	2.275	0.127	7.712	13.26	6.6	No
7148 Reinholdbien	2.286	0.099	5.641	13.14	5.2	No
8693 Matsuki	2.406	0.122	6.269	12.74	5.7	No
21238 1995 WV7	2.541	0.137	10.754	13.04	5.4	No

Table 2. Observational circumstances of the selected asteroids. The exposure time in seconds is derived by summing several acquisitions of each asteroid.

Asteroid	Date	RA	Dec.	Exposure time (s)
1929 Kollaa	2007/12/25	09 39 42.61	+24 37 37.6	480
1933 Tinchén	2007/12/25	07 12 06.99	+11 41 54.3	480
2011 Veteraniya	2007/12/25	01 40 57.06	+19 22 57.7	2400
2912 Lapalma	2007/12/26	12 00 56.95	+06 16 20.1	1440
3944 Halliday	2007/12/25	10 19 53.79	+20 04 02.7	2400
3968 Koptelov	2007/12/25	08 50 05.59	+20 27 25.7	2400
4147 Lennon	2007/12/25	04 05 57.90	+25 52 26.6	2400
4993 Cossard	2007/12/25	10 11 46.39	+21 48 37.7	1200
6406 (1992 MJ)	2007/12/25	09 33 05.83	+10 03 46.4	2400
7148 Reinholdbien	2007/12/25	01 04 55.00	+07 11 24.8	1200
8693 Matsuki	2007/12/25	04 06 16.53	+11 27 53.2	480
21238 (1995 WV7)	2007/12/25	03 10 43.36	+15 27 16.0	2400

the K filter (centred at 2.2 μm), centred in the expected RA and Dec. positions of the objects, according to the ephemeris generated from the NASA Horizons web site. The asteroids were identified as moving objects at the predicted position and with the predicted proper motion. The slit was oriented along the parallactic angle, and the tracking was at the object proper motion. Three well-known solar analogue stars (Land 115-27, Land 102-1081 and Hyades 64) were also observed during the night.

Each acquisition consists of a series of images in one position (position A) of the slit and then offsetting the telescope by 10 arcsec along the slit (position B), for a total exposure time as reported in Table 2, for each asteroid. This process was repeated and a number of ABBA cycles were acquired. This sequence makes the data reduction easier, as it allows a better estimate and removal of the sky contribution.

Data reduction was carried out according to reduction techniques described in Licandro, Ghinassi & Testi (2002), Duffard et al. (2004) and Lazzarin et al. (2004), for example. First of all, consecutive A and B pairs are subtracted, in order to remove the sky emission from both spectra, and divided by the flat-field. The master flat-field image is constructed from the flat-field images acquired in the *J*, *H*, *K* filters. Average flat-field images for each filter is derived, and then added to the master one, in the proper pixel position, according to the filter response. Each A–B frame had some residual of sky emission, related to sky transparency fluctuations and/or intrinsic variation of the airglow emission, which was eliminated by extracting the ‘short-slit’ spectrum around each A, B spectrum, then aligning and

combining them into the final short-slit spectrum from which the 1D spectra were extracted. Data were then compared with the solar analogue stars. Asteroid spectra are shifted with respect to stellar spectra, in order to locate the best superposition of the telluric bands observed in both spectra; finally asteroid reflectance is derived by dividing the asteroid spectrum by the star one. The asteroid spectra are finally normalized in order to have a reflectance value equal to 1 in the spectral range 1.5–1.7 μm .

3 ANALYSES OF THE SPECTRA

The NIR spectra thus obtained can then be analysed in terms of the mineralogical properties of the surface of the selected set of asteroids. The useful spectral range in the NIR region is 0.75–2.5 μm . The observed spectra for Vesta-family and non-Vesta-family asteroids are shown in Figs 1(a) and (b).

As one can see in Fig. 1, all the spectra are characterized by the typical absorption bands, near 1 and 2 μm , indicative of the presence of pyroxene. The spectrum of asteroid (6406) 1992 MJ A shows a band at 1.2–1.3 μm . The feature at $\sim 1.2 \mu\text{m}$ in pyroxenes, as well as in the HEDs, has been attributed to Fe^{2+} in the M1 crystallographic site in the pyroxene (Burns 1993; Sunshine & Pieters 1993; Klima, Pieters & Dyar 2008). This feature tends to be stronger for pyroxenes that cooled relatively quickly (Klima et al. 2008), which ‘traps’ some Fe^{2+} in the M1 crystallographic site.

All the observed asteroids have spectra typical of V-class asteroids. In order to visually compare all the spectra, these were

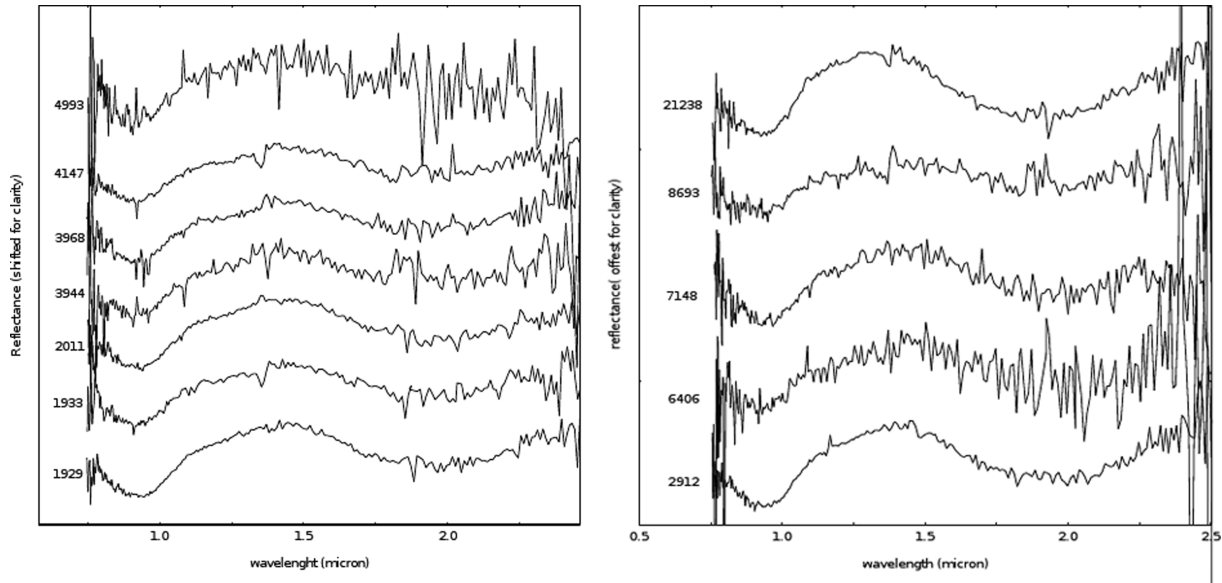


Figure 1. (a) Near-infrared spectra for the observed Vesta family asteroids. (b) Near-infrared spectra for the observed non-family V-type asteroids. All spectra are shifted on the vertical axis for clarity.

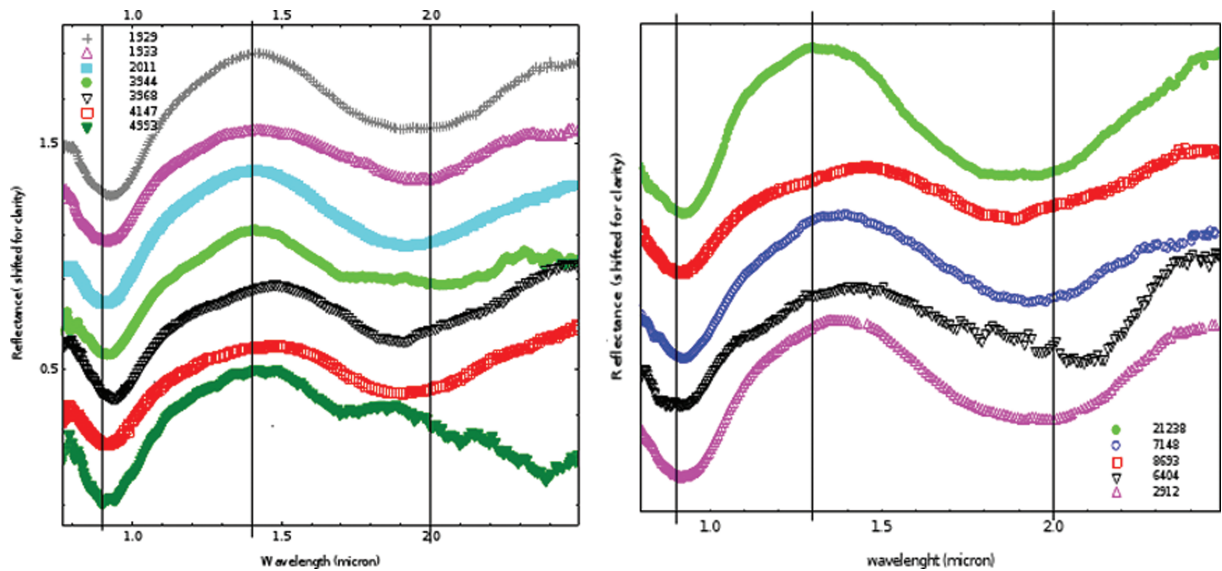


Figure 2. (a) Smoothed NIR spectra for the observed family V-type asteroids. (b) Smoothed NIR spectra for the observed non-family V-type asteroids. All spectra are shifted for clarity. Vertical lines at 0.9, 1.4 and 2.0 μm are plotted for reference.

smoothed and shown in Figs 2(a) and (b) for Vesta-family and non-family objects. Vertical lines at 0.9, 1.4 and 2.0 μm are shown for reference.

In Fig. 2(a), it can be noted that the spectrum of asteroid (4993) Cossard is quite different from the other spectra, with an anomalous decay in reflectance around and after 2.0 μm . We believe this decay is not real but due to some instrumental and/or observational error. We give the spectrum here just for comparison, but the values computed from it must be taken with concern.

Several parameters, such as band minima, centre, depth, width and area, have been traditionally used to infer the asteroid's mineralogy (see Adams 1974; Gaffey et al. 2002; Sunshine & Pieters 1993 for a detailed review on the topic). Among these, the most important are related to the centre of the absorption band near 1 and 2 μm , or band I and band II (hereafter BI and BII, respectively), in

particular the band minimum and the band centre. These are defined as the wavelength position of the point of lowest reflectance before and after the removal of the continuum, respectively (Cloutis & Gaffey 1991). The continuum, on the other hand, is defined by the linear fit between the maxima near 0.7, 1.4 and 2.4 μm .

It is important to note that to apply this technique we need a spectrum that encompasses the two maxima, at 0.7 and 1.4 μm . However, it is usually necessary to join two spectra taken at different instants since the V and IR spectra are never obtained simultaneously. This is not a problem if we take spectra of a sample (meteorite or mineral assemblage) in the laboratory, because the overlapping region between the two spectra has been acquired in the same observational conditions. In the case of ground-based observations, however, we can only guarantee that we are observing the same illuminated region of the object

Table 3. Spectral parameters of the selected sample of V-type asteroids.

Asteroid	BI min (μm)	BII min (μm)	BI centre (μm)	BII centre (μm)	Band separation (μm)
Vesta family asteroids					
1929	0.923 ± 0.004	1.947 ± 0.005	0.930 ± 0.004	1.954 ± 0.005	1.025 ± 0.009
1933	0.915 ± 0.004	1.936 ± 0.006	0.922 ± 0.004	1.943 ± 0.006	1.022 ± 0.011
2011	0.921 ± 0.005	1.956 ± 0.008	0.928 ± 0.005	1.963 ± 0.008	1.035 ± 0.013
3944	0.912 ± 0.002	1.943 ± 0.02	0.919 ± 0.002	1.950 ± 0.02	1.030 ± 0.022
3968	0.920 ± 0.005	1.922 ± 0.02	0.927 ± 0.005	1.929 ± 0.02	1.002 ± 0.025
4147	0.919 ± 0.003	1.926 ± 0.005	0.926 ± 0.003	1.933 ± 0.005	1.007 ± 0.013
4993	0.921 ± 0.003	2.071 ± 0.02	0.928 ± 0.003	2.078 ± 0.02	1.151 ± 0.023
Non-Vesta family asteroids					
2912	0.922 ± 0.003	1.932 ± 0.01	0.929 ± 0.003	1.939 ± 0.01	1.010 ± 0.013
6406	0.916 ± 0.003	1.990 ± 0.02	0.923 ± 0.003	1.997 ± 0.02	1.074 ± 0.023
7148	0.923 ± 0.003	1.948 ± 0.02	0.930 ± 0.003	1.955 ± 0.02	1.025 ± 0.023
8693	0.892 ± 0.005	1.923 ± 0.02	0.899 ± 0.005	1.930 ± 0.02	1.031 ± 0.025
21238	0.908 ± 0.002	1.900 ± 0.005	0.915 ± 0.002	1.907 ± 0.005	0.992 ± 0.007

if we know its rotational properties, in particular the period and the direction of the pole. Unfortunately, these data are known only for a very small number of asteroids, mostly the largest ones. Therefore, the commonly used technique of joining the visible spectra obtained from available data sets (such as SMASS and S3OS2) with the NIR can introduce significant errors in the determination of BI centre. It is important to mention that differences in the observational configuration of the asteroid such as the rotational phase, the aspect angle, the solar phase and the airmass can give rise to changes in the slope of the spectrum affecting, therefore, the reliability in the determination of the BI centre. For this reason, in the following we will just compute band minima and use laboratory determinations to derive the band centre, as explained in Section 3.1.

3.1 Spectra analysis

Using the full NIR spectra, we determined the position of the two minima near 0.9 and 2.0 μm . These values have been calculated by fitting a second-order polynomial to the spectral curve in a small region of the minimum. We always fit the spectral region between 0.8 and 1.1 μm for BI and between 1.6 and 2.3 μm for BII. The error in the position of the minimum has been obtained through the errors of the coefficients of the fitted parabola.

We choose to evaluate the band centres using the simple relations between band minima and band centre found by Cloutis & Gaffey (1991). Therefore, in principle it is possible to compute the band centres and, consequently, the [Wo] and [Fs] contents, when the spectrum does not encompass the peak at 0.7 and the two bands. Band separation is defined as the difference between BII and BI minima. In Table 3, we list all the computed parameters.

Each of the above computed spectral parameters is diagnostic of the associated mineralogy present on the surface of the observed asteroids. The relationship between these spectral parameters and the mineralogy of the sample observed, particularly pyroxene and olivine, has been studied in various papers over the last years (Adams 1974, 1975; King & Ridley 1987; Cloutis & Gaffey 1991) and recently reviewed by Gaffey et al. (2002). In the following section, we will discuss the different mineralogical properties of the observed asteroids as disclosed by the computed spectral parameters.

3.2 Inferred mineralogy

As stated above, band centres are among the most important diagnostic parameters of the mineralogy in a spectrum. According to several authors (Gaffey 1976; Adams 1974; Cloutis & Gaffey 1991) in most pyroxenes and in the basaltic achondrites, there is a strong correlation between the position of BI centre and BII centre and the associated mineralogy. For example, orthopyroxene bands shift to longer wavelengths with increasing amounts of iron, whereas clinopyroxene bands shift to longer wavelength with increasing calcium content.

Depending on their petrogenesis, mafic rock assemblages (as pyroxene) commonly contain either a pyroxene of a single composition or two coexisting pyroxene compositions. It is very difficult to distinguish the presence of one or two pyroxenes from the spectra, without a careful spectral analysis based primarily on Modified Gaussian Model (MGM) (Sunshine & Pieters 1993). Although assemblages containing a single pyroxene species are found in nature, it is quite common to find assemblages with two or more coexisting pyroxenes. In these cases, the position of the absorption features in the reflectance spectrum is a weighted average of the positions of the bands arising from each individual pyroxene phase.

The compositions of HED pyroxenes reported in the literature are commonly of the bulk phase including two pyroxenes – a low-calcium orthopyroxene phase hosting small high-calcium augite exsolution lamellae. The primary mineral of diogenites is orthopyroxene (92–95 per cent), while the main pyroxene found in eucrites is pigeonite. Thus, the spectral derived composition of HED corresponds to the analytical compositions, giving an average of the two pyroxenes present in the sample.

Diogenites and basaltic eucrites can be quite easily distinguished from one another spectrally on the basis of the position of the 1 and 2 μm bands, which move to longer wavelengths with the addition of Fe^{2+} and/or Ca. It is much more difficult to distinguish HEDs of similar bulk composition but different cooling history, such as the basaltic eucrites and cumulate eucrites, using only the 1 and 2 μm bands positions.

In Fig. 3, the values of BI versus BII centres for the observed asteroids are shown. Here, and in the subsequent figures, we will not include the values for asteroid (4993) Cossard due to the above-mentioned problem with its spectrum.

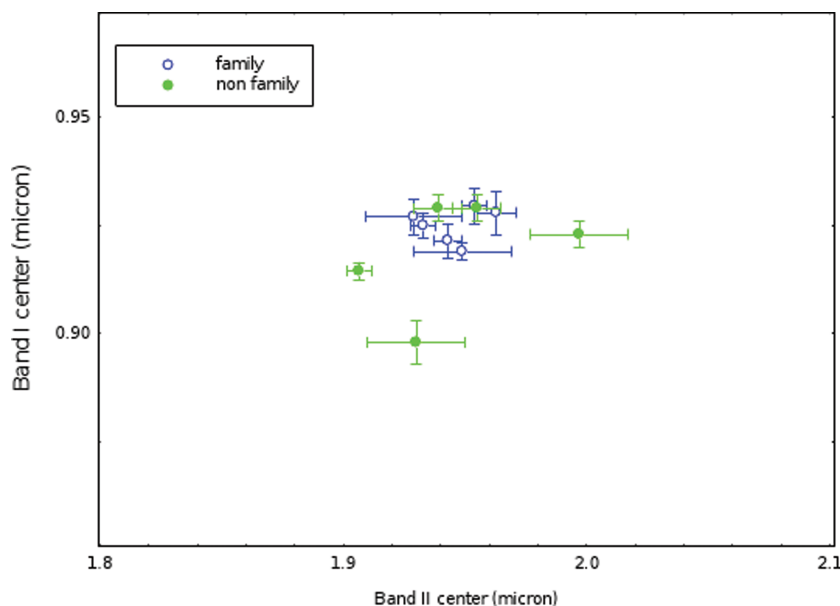


Figure 3. Values of BI centre versus BII centre for the observed sample of asteroids. Vesta family asteroids and non-Vesta family asteroids are marked in different colours: blue open points – family members; green filled points – non-family members.

The pyroxene composition, i.e. the molar Ca, [Wo] and Fe, [Fs], contents can be obtained from the values of the absorption band centres near 1 and 2 μm using equations derived by exhaustive laboratory calibrations performed by several authors (Adams 1974, 1975; King & Ridley 1987; Cloutis & Gaffey 1991; Burbine et al. 2007). These equations have been recompiled by Gaffey et al. (2002) for pyroxenes and by Burbine et al. (2007) for HED meteorites and are here used to derive the [Wo] and [Fs] contents for our sample of asteroids. These equations work well for the spectra of pure pyroxene samples, for spectra of mixtures of olivine and orthopyroxene and for spectra of HED meteorites (Gaffey 2007). The Burbine et al. (2007) formulae only work on the very restricted pyroxene mineralogies found in HEDs whereas the Gaffey et al. (2002) formulae work on a much wider range of pyroxene mineralogies.

The errors obtained with these formulae are of the order of ± 4 –5 per cent according to Gaffey et al. (2002), and ± 1 –4 per cent according to Burbine et al. (2007). Each formula provides a slightly different value, so we listed in Table 4 the maximum and minimum values for [Wo] and [Fs] contents obtained using formulae mentioned above. However, the possible ranges for the calculated [Fs] and [Wo] contents can be larger than the given uncertainties for the formulae if the band position uncertainty is large.

In Table 4, we listed maximum and minimum values for [Wo] and [Fs] contents, obtained using Gaffey et al. (2002) and Burbine et al. (2007) formulae.

There are small differences in the results obtained using the formula derived by Gaffey et al. (2002) and that of Burbine et al. (2007). The former gives larger values of [Wo] and [Fs] contents than the latter. In any case, all the analysed objects have low-calcium content pyroxenes, as indicated by a [Wo] value less than 10; this would imply a higher content of orthopyroxene. For the asteroid (4993) Cossard, using equations based on the position of BII, the computed [Fs] content is greater than 50, well outside the validity range of the Gaffey et al. (2002) equations. The spectrum of this asteroid at wavelength longer than 2 μm must be taken with caution, because of the above-mentioned problems. For this reason, for (4993) Cossard we reported only the values computed using the 1 μm band with the formal errors as given in Burbine et al., (2009). Asteroids (6406)

Table 4. Molar contents for the observed asteroids.

Asteroid	[Wo]	[Fs]
Vesta family asteroids		
1929	7–8.5	36.3–40.3
1933	4.4–6.5	28.9–37.4
2011	6.9–7.9	35.5–42.7
3944	3.6–6.8	26.6–39.2
3968	5.2–7.6	31.2–33.6
4147	5.5–6.8	32.0–34.7
4993*	5.8–7.8	32.0–38.0
Non-Vesta family asteroids		
2912	5.9–8.2	33.3–36.3
6406	5.0–10.6	30.4–51.8
7148	7.2–8.5	36.6–40.6
8693	0–5.0	5.5–33.9
21238	1.6–3.4	21.7–27.6

*For the asteroid (4993) Cossard we reported only the values computed using the 1 μm band with the formal errors as given in Burbine et al. (2009), due to the low signal-to-noise ratio (S/N) in the 2 μm band region.

1922 MJ and (8693) Matsuki show large differences in [Wo] and [Fs] if BI or BII are used to compute those values. The spectrum of (6406) 1922 MJ has a quite unusual BII profile, probably due to the low S/N in that range, while (8693) Matsuki shows a BI centre located at very low wavelengths. In both cases, we think that the variations in molar content are due to a non-optimal band centre evaluations.

The band separation versus BII plot can also be used to estimate the iron content in orthopyroxenes (Cloutis et al. 1990). A very clear linear trend emerges from laboratory data: both parameters, band separation and BII, increase with growing iron content (Cloutis 1985). Similar linear trend appears when we plot the values of these parameters for our sample, as can be seen in Fig. 4.

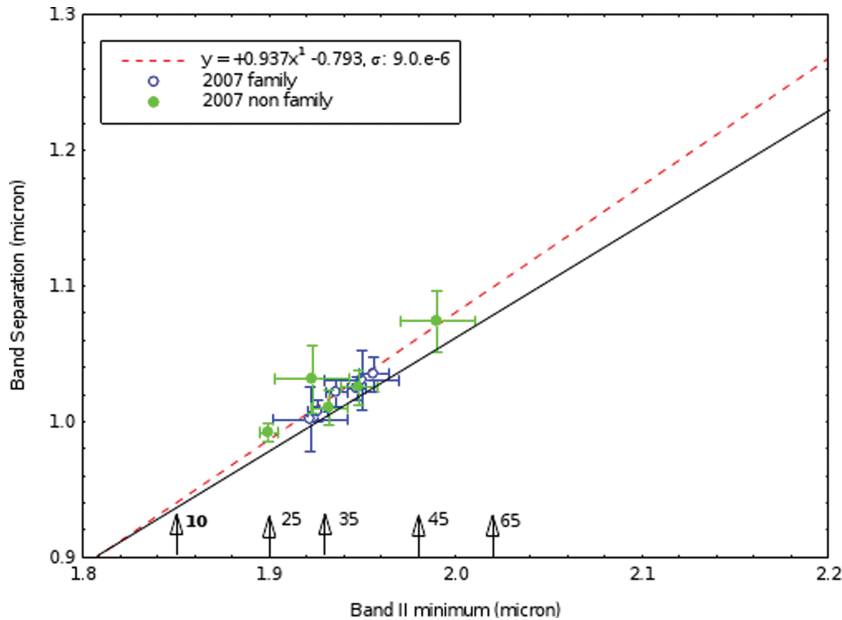


Figure 4. Band separation versus BII minimum. The arrows along the horizontal axis indicate the iron content (mole per cent ferrosilite). Vesta family asteroids and non-Vesta family asteroids are marked in different colours: blue open points – family members. Green filled points – non-family members. The dashed line represents a linear least-squares fit to our data while the solid line reproduces the value given by Cloutis et al. (1990).

In this figure, the red dashed line represents a linear least-squares fit to our data. The solid line reproduces the one given by Cloutis et al. (1990) for a suite of pyroxene compositions. As can be seen, all asteroids lie on a line, with the exception of (8693) Matsuki that is located slightly above the line.

4 RE-ANALYSIS OF THE PREVIOUS PUBLISHED DATA

A reassessment of previously published data (Duffard et al. 2004) has also been performed using the above-described method. The original analysis was based on combining visible and NIR spectra for the same object, but taken at different times without consideration of differences in geometry or rotational phase of the observations, and hence deviations from results obtained with the method described in the present paper are expected. Therefore, we decided to re-analyse the data published in Duffard et al. (2004) using only

the infrared part of the spectrum (from 0.7 to 2.5 μm) so that it can be directly compared to the new data presented here. In Table 5, we list the obtained parameters.

In Fig. 5, we plot the band minima obtained with the new methodology for the overall data set. Here, and in the subsequent figures, as well as in the analysis, we will not include the values for asteroid (10285) 1982QX1 due to the low S/N of its spectrum at 2 μm . The V symbols indicate (4) Vesta from Gaffey (1997) (two points that represent the maximum and the minimum values of the band positions over a rotational period with the associated errors) and Vernazza et al. (2005).

The objects observed in the present work have the tendency to occupy the region with slightly smaller values of BI centre with respect to Vesta, as can be observed in Fig. 5.

In Fig. 6, the band separation for the whole data set is plotted. The dispersion of the data is much smaller and the band separation fit is very good, with respect to the previous analysis (Duffard et al. 2004).

Table 5. Spectral parameters of the asteroid sample presented in Duffard et al. (2004).

Asteroid	BI min	BII min	BI centre	BII centre	Band separation	Vesta family
809 Lundia	0.923 ± 0.005	1.935 ± 0.03	0.930 ± 0.005	1.942 ± 0.03	1.012 ± 0.035	No
956 Elisa	0.912 ± 0.003	1.912 ± 0.03	0.919 ± 0.003	1.919 ± 0.03	1.00 ± 0.033	No
2468 Repin	0.922 ± 0.004	1.93 ± 0.03	0.929 ± 0.004	1.937 ± 0.03	1.008 ± 0.034	Yes
2763 Jeans	0.923 ± 0.003	1.957 ± 0.03	0.930 ± 0.003	1.964 ± 0.03	1.034 ± 0.033	No
2851 Harbin	0.91 ± 0.003	1.904 ± 0.03	0.917 ± 0.003	1.911 ± 0.03	0.994 ± 0.033	No
3268 De Sanctis	0.91 ± 0.004	1.976 ± 0.02	0.917 ± 0.004	1.983 ± 0.02	1.066 ± 0.024	Yes
3498 Belton	0.92 ± 0.005	1.968 ± 0.03	0.927 ± 0.005	1.975 ± 0.03	1.048 ± 0.035	Yes
3782 Celle	0.927 ± 0.01	1.951 ± 0.01	0.934 ± 0.01	1.958 ± 0.01	1.024 ± 0.011	Yes
4796 Lewis	0.919 ± 0.005	1.935 ± 0.03	0.926 ± 0.005	1.942 ± 0.03	1.016 ± 0.035	No
4815 Anders	0.931 ± 0.005	1.96 ± 0.03	0.938 ± 0.005	1.967 ± 0.03	1.029 ± 0.035	Yes
6631 1992 FZ1	0.912 ± 0.004	1.972 ± 0.03	0.919 ± 0.004	1.979 ± 0.03	1.06 ± 0.034	Yes
10285 1982 QX1	0.921 ± 0.003	2.077 ± 0.02	0.928 ± 0.003	2.084 ± 0.02	1.156 ± 0.023	Yes
10320 1990 TR1	0.917 ± 0.005	2.021 ± 0.03	0.924 ± 0.005	2.028 ± 0.03	1.104 ± 0.035	Yes
10349 1992 LN	0.911 ± 0.003	1.923 ± 0.01	0.918 ± 0.003	1.93 ± 0.01	1.012 ± 0.013	Yes

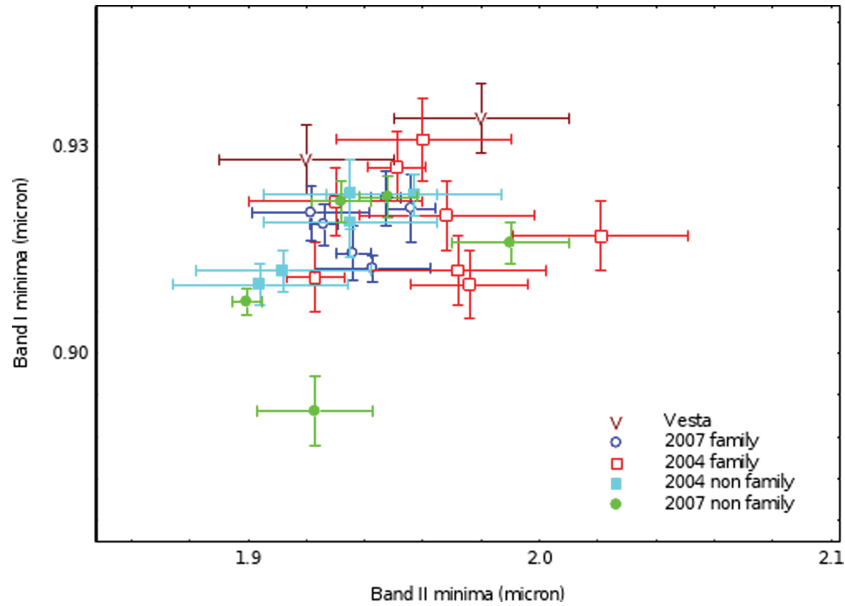


Figure 5. Values of BI minima versus BII minima for the total sample of observed asteroids. The V symbols indicate (4) Vesta from Gaffey (1997) (the points represent the maximum and the minimum values over a rotational periods with the associated errors) and Vernazza et al. (2005). Vesta family asteroids and non-Vesta family asteroids are marked differently: open points – family members; filled points – non-family members.

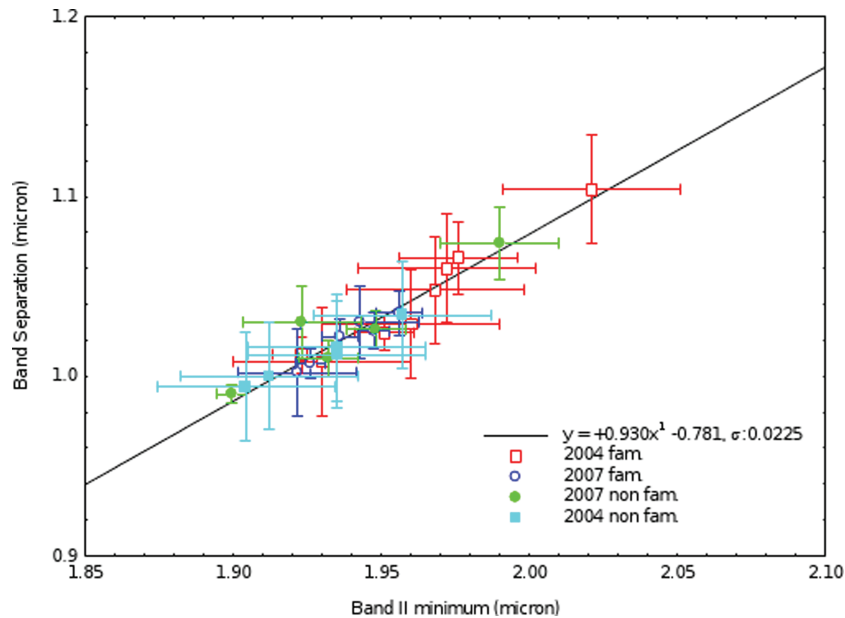


Figure 6. Band separation versus BII minimum. Open and filled points represent asteroids that are members and non-members of the Vesta dynamical family, respectively. The solid line represents a linear least-squares fit to our data.

We computed [Wo] and [Fs] contents using the above-mentioned formulae (Gaffey et al. 2002; Burbine et al. 2007) and the resulting values are reported in Table 6.

5 BAND ANALYSIS OF HED METEORITES

The HED meteorites comprised diogenites (orthopyroxenites), basaltic and cumulate eucrites (basalts and gabbros), and howardites (regolith breccias composed primarily of eucrites and diogenites). HED meteorites are believed to come from Vesta or smaller asteroids that are spectrally similar to Vesta and could be collisionally derived pieces of Vesta (Vestoids). The mineralogical analysis of

Vestoids should be compared with HEDs composition. The method described in the previous paragraph for the V-type asteroids is applied to the HEDs spectra and the results are described below. For completeness, a quick description of the mineralogy of HED meteorites is provided.

Diogenite meteorites are mainly composed of orthopyroxenes (for the 87–99 per cent) with a few per cent of olivine (less than the 10 per cent). Diogenites are quite homogeneous in major element composition, especially for Mg and Fe, which vary in the range $Wo_{1-3} En_{71-77} Fs_{22-24}$ (Fowler et al. 1994; Mittlefehldt 1994). A special class of diogenites, called ‘olivine diogenites’, shows a significant amount of olivine in their composition (Sack et al. 1991).

Table 6. [Wo] and [Fs] molar contents.

Asteroid	[Fs]	[Wo]
Vesta family		
2864	29.7–33.9	5.3–5.9
3268	17.5–46.6	0.3–9.5
3948	27.7–44.1	4.5–8.9
3782	34.8–39.5	6.6–7.5
4815	38.9–41.9	8.3–9.1
6631	19.5–45.2	1.1–9.2
10320	24.6–58.3	3.2–13.1
10349	18.5–32.0	0.7–5.3
Non-Vesta family		
809	30.8–35.2	5.7–6.3
956	19.5–29.1	1.1–4.5
2763	30.8–41.2	5.7–8.0
2851	17.4–26.9	0.3–3.8
4796	26.7–35.3	4.1–6.3

We listed here the maximum and minimum values for [Wo] and [Fs] contents obtained using Gaffey et al. (2002) and Burbine et al. (2007) formulae.

However, many other minerals were found to be included in some part in the olivine-bearing diogenites, like harzburgite, which is composed of olivine plus magnesian orthopyroxene rocks (Beck & McSween 2010). Their spectra tend to have band centres at shorter wavelengths than howardites and eucrites as they contain pyroxenes with a low-calcium composition.

Eucrites are mainly made of pyroxene (ortho and clinopyroxenes) and plagioclase, with ilmenite, apatite and quartz in minor amounts. Following a petrological classification, eucrites are divided in basaltic or cumulate rocks. Most of the basaltic eucrites are brecciated, composed of fine to medium grains; however many samples show a wide variety of different textures. The cumulate eucrites, on the other hand, are predominantly unbrecciated (Mittlefehldt et al. 1998), though some clasts were identified within polymict eucrites (Takeda & Graham 1991; Lindstrom & Mittlefehldt 1992). The most probable origin of these meteorites is from crystallization as lavas on the surface of the asteroid or within relatively shallow level dikes and plutons. Eucrite have distinctive absorption features near 1 and 2 μm due to the pyroxenes. The positions of these bands are directly proportional to the cations in the octahedral sites: both 1 and 2 μm bands shift to longer wavelengths with an increase in calcium content (Adams 1974; Burns 1993). Band shift to longer wavelengths can be attributed to the presence of trivalent phases such as Fe^{3+} , Al^{3+} and Ti^{3+} (Adams 1974).

Howardites are mixtures of eucritic and diogenitic clasts. The igneous clasts found in the howardites are quite similar to the mineralogy of the unbrecciated eucrites, though exceptions were found on individual meteorites (Delaney, Prinz & Takeda 1984; Bunch & Rajan 1988; Mittlefehldt et al. 1998). They are thought to come from an impact event, which may have produced igneous clasts in howardites; the solar-type noble gases enrichment on the surface of mineral and glass fragments also testify this. Ground-based spectroscopic investigation (Binzel et al 1997; Gaffey 1997) suggests that much of Vesta surface is similar to the chemical composition and mineralogy of howardites.

For a more complete description of the HED suite, please refer to McSween et al. (2010) and references therein.

Because it is believed that V-type asteroids could be progenitors of HEDs we decided to analyse the HEDs mineralogy with the same

methods used for the Vestoids looking for correlations, analogies and similarities. We performed a spectral band analysis for some HED meteorites that are included in the Brown RELAB spectral catalogue (RELAB; <http://www.planetary.brown.edu/rehab/>; Pieters & Hiroi 2004). In Table 7, the HED samples analysed are listed. We selected HED spectra of powders of grains size below 25 μm , because it is believed that the grains that compose the regolith of Vestoids are of the order of 25 μm in size or less (Hiroi et al. 1994, 1995). In this analysis of HED spectra we do not want to perform a detailed study of spectral changes as a function of particle size or other effects, such as irradiation. We refer to Duffard, Lazzaro & de León (2005) for this grain size effects on HED band parameters.

We derived the band parameters applying the same method used for the V-type asteroids, in order to have a fully comparable data set. A plot of BI centre versus BII centre for the HEDs is shown in Fig. 7. The three HED subgroups lie in different portions of the plot with a small overlap at the boundaries between different regions. Each meteorite subgroup has been marked with different colours so that they can be compared to the band parameters of the V-type asteroids of this study.

The eucrites of the examined sample tend to have band centres at longer wavelengths than the diogenites, while the howardites lie in the intermediate region between the two subgroups. The BI versus BII distribution of the HED has been previously addressed (Gaffey 1997; Duffard et al. 2005) and the results here confirm the previous analysis: the absorption bands are at shorter wavelengths for diogenites, and longer for the howardites and eucrites.

The [Wo] and [Fs] contents of the HED sample are derived from the equations compiled by Gaffey et al. (2002) and Burbine et al. (2007) and reported in Table 7. The retrieved minimum and maximum values are listed, according to the previous discussion.

All the derived mineralogies from the two sets of equation overlap: the derived [Wo] contents are almost exactly the same with differences of about 1–2 mol per cent, while the derived [Fs] contents are larger with differences up to 8 mol per cent. However, the differences reported for meteorite samples are not large as for the asteroid sample. This is due to the larger errors in the spectra of the asteroids, especially in the 2 μm region, where the noise could be quite large.

The measured ranges of the average [Fs] and [Wo] contents of pyroxene (Mittlefehldt et al. 1998, Berkley & Boynton 1992, Takeda 1997) are for the eucrites: [Fs] \sim 30–55 and [Wo] \sim 6–15; howardites: [Fs] \sim 31–42 and [Wo] \sim 4–8; diogenites: [Fs] \sim 20–30 and [Wo] \sim 1–3. Hence, we can say that the values obtained using the above-mentioned equations are in the ranges of the real ones, considering the declared errors of ± 5 for [Fs] and ± 3 for [Wo].

6 DISCUSSION

6.1 Comparison of the spectral parameters of HEDs, Vestoids and (4) Vesta

The spectral parameters obtained in the section before can be directly compared with results of Gaffey (1997) for the asteroid 4 Vesta and with parameters here derived for the V-type asteroids. Figs 7(a) and (b) show the calculated [Fs] and [Wo] contents for the V-type asteroids versus the ranges found for the HEDs listed in Table 7.

From the comparison of these asteroids with the average HED, it seems that the observed objects have an average [Fs] and [Wo] contents consistent mainly with howardites and diogenites, suggesting

Table 7. Band parameters and derived molar content of HED meteorites.

Meteorite	Subgroup	BI centre (μm)	BII centre (μm)	[Wo]	[Fs]
Binda	Howardite	0.928	1.95	7.0–7.8	36.7–38.7
Bununu	Howardite	0.928	1.95	7.0–7.8	37.3–39.5
EET83376	Howardite	0.934	1.98	9.4–10.3	43.5–47.6
EET87503	Howardite	0.929	1.97	7.4–8.2	41.2–44.6
EET87513	Howardite	0.932	1.98	8.6–9.5	42.4–46.2
Frankfort	Howardite	0.927	1.94	6.6–7.4	36.1–37.9
GRO95535	Howardite	0.929	1.96	7.4–8.2	39.8–42.7
Kapoeta	Howardite	0.928	1.94	7.0–7.8	34.2–35.5
Le-Teilleul	Howardite	0.928	1.94	7.0–7.8	35.7–37.4
Petersburg	Howardite	0.934	1.99	9.4–10.3	44.9–49.5
QUE94200	Howardite	0.921	1.93	4.2–4.9	32.2–32.8
Y7308	Howardite	0.927	1.94	6.6–7.4	35.5–37.1
Y790727	Howardite	0.931	1.96	8.2–9.0	40.0–43.0
Y791573	Howardite	0.926	1.95	6.2–7.0	36.7–38.7
A87272	Eucrite	0.941	2.03	12.2–13.2	53.9–60.4
A881819	Eucrite	0.931	1.97	8.2–9.1	42.5–46.2
ALH78132	Eucrite	0.933	1.97	9.0–9.9	40.6–43.8
ALH85001	Eucrite	0.925	1.95	5.8–7.5	37.5–39.8
ALHA76005	Eucrite	0.935	1.99	9.8–10.7	46.6–51.6
Bouvante	Eucrite	0.936	2.03	10.2–11.2	53.6–60.7
Cachari	Eucrite	0.94	2.02	11.8–12.8	52.9–59.9
EET90020	Eucrite	0.941	2.01	12.2–13.2	49.9–55.9
EETA79005	Eucrite	0.934	1.97	9.4–10.3	42.1–45.7
GRO95533	Eucrite	0.941	2.04	12.2–13.2	55.6–63.4
Ibitraa	Eucrite	0.94	2.00	11.8–12.8	47.4–52.7
Jonzac	Eucrite	0.939	2.01	11.4–12.4	50.1–56.1
Juvinas	Eucrite	0.936	2.00	10.2–11.2	48.1–53.5
LEW85303	Eucrite	0.945	2.02	13.8–14.9	51.9–58.8
LEW87004	Eucrite	0.934	1.96	9.4–10.3	39.8–42.8
Millbillillie	Eucrite	0.938	2.02	11.0–12.0	51.3–57.8
Moore County	Eucrite	0.938	1.99	11.0–12.2	44.7–49.2
NWA011	Eucrite	0.95	2.03	15.7–17.0	53.4–60.4
Padvarninkai	Eucrite	0.939	2.01	11.4–12.4	49.9–55.9
Pasamonte	Eucrite	0.939	2.00	11.4–12.4	48.1–53.5
Serra de Mage	Eucrite	0.931	1.97	8.2–9.1	42.1–45.7
Stannern	Eucrite	0.933	2.02	9.0–9.9	50.9–57.2
Y74450	Eucrite	0.934	1.97	9.4–10.3	41.2–44.6
Ellemeet	Diogenite	0.92	1.90	3.8–4.4	26.1–27.1
Johnstown	Diogenite	0.914	1.87	1.5–1.9	21.4–18.9
Y74013	Diogenite	0.92	1.92	3.8–4.5	30.7–30.9
Y75032	Diogenite	0.922	1.92	4.6–5.1	29.7–31.3
EETA7092	Diogenite	0.919	1.91	3.5–4.1	28.8–28.3
GRO95555	Diogenite	0.92	1.92	3.9–4.5	30.7–30.9

The maximum error associated with BI and BII evaluations are respectively 0.002 and 0.01

that some of them reflect a mixture of diogenite and eucrite materials. None the less, it is also evident that none of the observed Vestoids has [Fs] and [Wo] content consistent with only eucritic material, while some are consistent only with diogenitic material.

Some asteroids show a very large range of possible average pyroxene content, compatible with mineralogies of the three HEDs subgroups. The spectrum of asteroid (10320) Reiland shows low S/N in the 2 μm band region, so the very large range of [Wo] and [Fs] content could be due to a poor determination of the BII centre [BII centre is required in Gaffey et al. (2002) equation]. Similarly, asteroid (8693) Matsuki has BI at 0.899 μm , while BII is at 1.93 μm , determining the large range of pyroxene content.

More in general, the Gaffey et al. (2002) and Burbine et al. (2007) formulae applied to ground-based spectra almost always give different values, and it is not easy to recognize which formula is the one that is more suitable to infer the mineralogical composition

of the Vestoids. These formulae work well for laboratory spectra with very high S/N, for which it is quite easy to determine the pyroxenes bands position with small errors. In case of asteroids spectra, especially for those quite faint, it is difficult to determine the exact band position, and the spectral analysis is often affected by large errors.

Looking at Fig. 7, we see that for some objects, the ranges of the calculated mineralogies tend to encompass the eucrite, howardite and diogenite ranges, like the case of asteroid (10320) Reiland. However, these asteroids have quite noisy spectra, and it is difficult to understand their mineralogies. On the other hand, there are some asteroids that show a narrower range of possible mineralogies. They have [Fs] and [Wo] contents consistent mainly with diogenites and howardites.

In Fig. 8, we plot the asteroid band centres and the HED band centres. We derived the band centres from RELAB spectra of HED

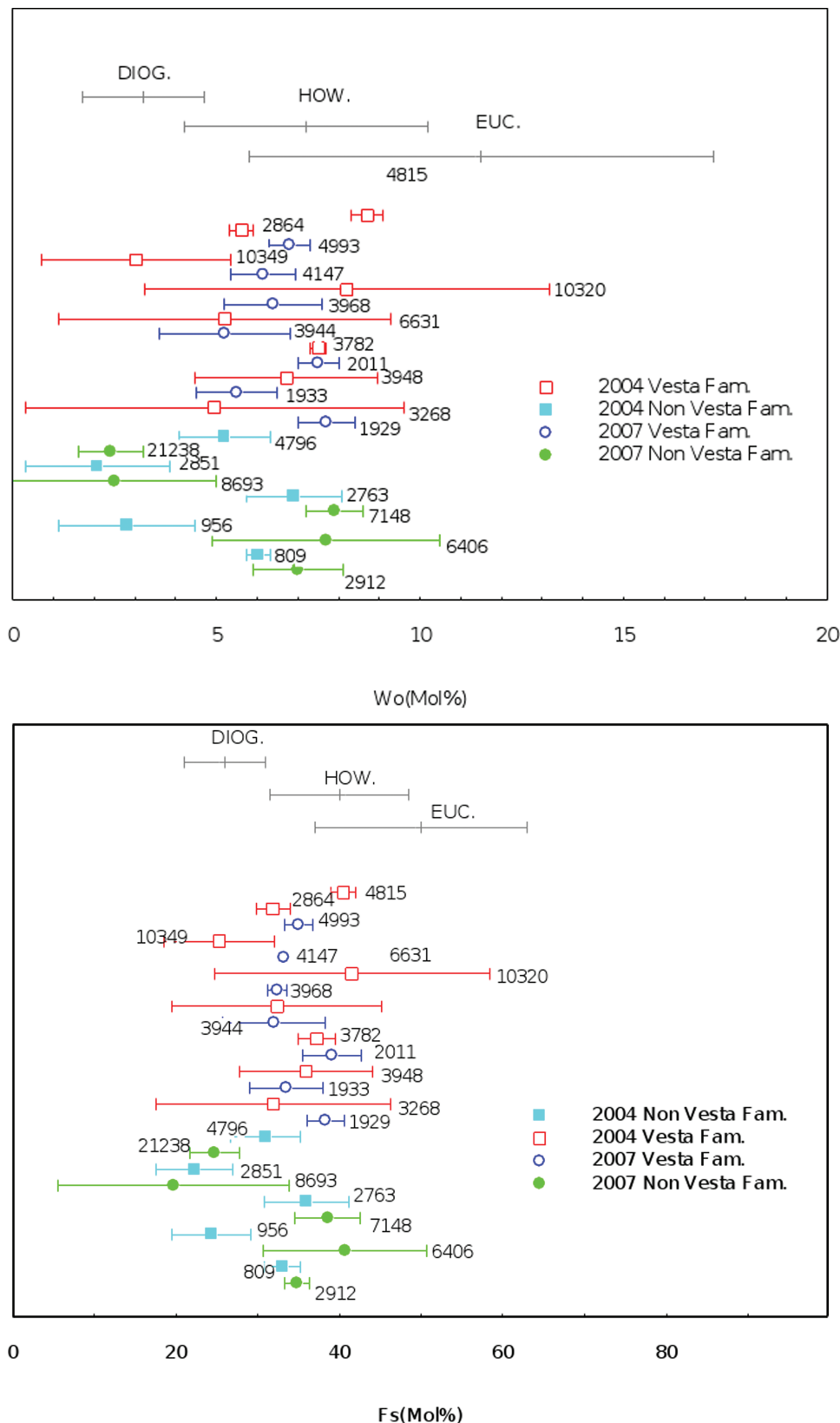


Figure 7. (a) Plot of wollastonite [Wo] ranges for the eucrites, howardites and diogenites here derived in comparison with [Wo] ranges derived for the Vestoids. The [Wo] ranges have been derived using Gaffey et al. (2002) and Burbine et al. (2007) equations. Vesta family asteroids and non-Vesta family asteroids are marked differently: open marks – family members; filled marks – non-family members. (b) Plot of ferrosilite [Fs] ranges for the eucrites, howardites and diogenites here derived in comparison with [Fs] ranges derived for the Vestoids. The [Fs] ranges have been derived using Gaffey et al. (2002) and Burbine et al. (2007) equations. Vesta family asteroids and non-Vesta family asteroids are marked differently: open marks – family members; filled marks – non-family members.

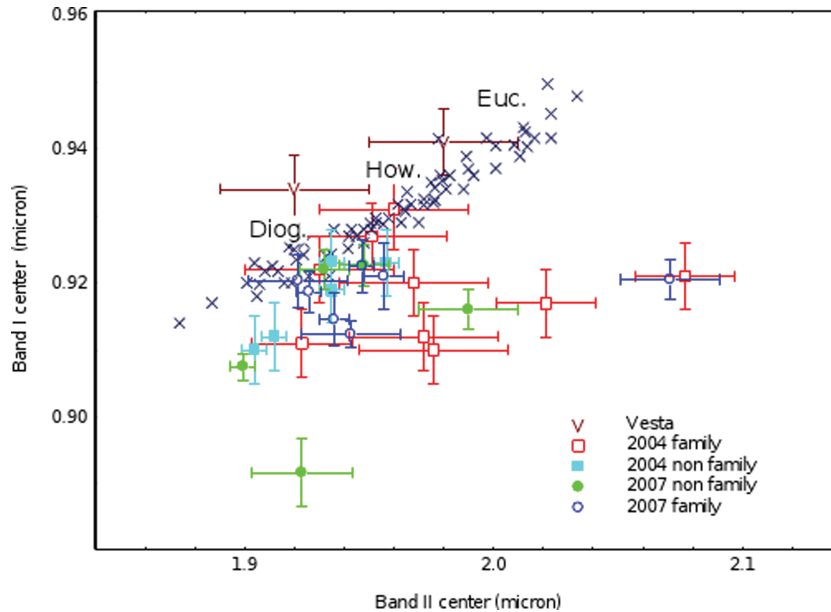


Figure 8. Values of BI centre versus BII centre for our sample of Vestoids and for HEDs (as listed in Table 7). Open and filled symbols represent asteroids that are members and non-members of the Vesta dynamical family, respectively. The V symbols indicate (4) Vesta: black from Gaffey 1997 (the two points represent the maximum and the minimum values over a rotational periods with the associated errors), blue from Vernazza et al. (2005).

meteorites (see Table 7) selecting spectra of HED powders with grain size below 25 μm .

From the analysis of this figure it seems that while (4) Vesta (values from Gaffey 1997 and Vernazza et al. 2005) lies in the region between diogenites and eucrites (mainly howardites region) most of the objects observed in the present work have a tendency to occupy the region with smaller values of BI centre. Vesta, however, seems to have a quite large spectral variability according to the plot of BI versus BII from Gaffey (1997) and Vernazza et al. (2005). The Gaffey's data of Vesta seem to be slightly over the region of the HEDs here plotted, while the Vernazza data are similar to HEDs data and similar to the values of Vestoids examined here.

Several asteroids plot in a region quite distinct from the HEDs. Most of the observed Vestoids show a low level of Ca content (<10 per cent Wo) (see Tables 4 and 6). This result implies that none of the Vestoids studied consists of just eucritic material but must contain a diogenitic component. The diogenites are orthopyroxenes, and therefore contain Ca-poor (low Wo) pyroxenes.

This finding is consistent with the work by Mayne et al. (2007), where none of the observed 15 V-type asteroids consists entirely of eucritic material but the studied V-types have at least some diogenitic component. They conclude that hemispheric averaging of eucrite and diogenite terrain would drive the average pyroxene composition to lower [Wo] values, as observed for such V-type asteroids; alternatively, some of the Vestoids may consist of material that is predominantly howardite at a fine-scale, which would result in a mixed spectrum. Shestopalov et al. (2010) found that the range of spectral parameters of the HEDs covers a wider region of parameter space than the disc-integrated asteroids and Vesta. According to their analysis, Vesta surface is more uniform than most Vestoids and HEDs and, moreover, the Vesta surface material is slightly different from that of Vestoids and HEDs. The spectral diversity between Vesta, V-type asteroids and HEDs has been recently addressed by Marchi et al. (2010) that found large differences in their spectral slopes.

The fact that V-type asteroids and HED band parameters do not overlap must be analysed with attention. The origin of this offset is unclear: several effects can concur to give these results such as differences between the asteroidal and laboratory environments, composition, space weathering or instrumental systematic. Here, we have decided for the use of only NIR range in order to have a fully consistent data set. On the other hand, the NIR range does not permit to evaluate the band centre in a classical way, removing the continuum from the spectra. We estimated the band centres adding the constant value +0.007, which is the one obtained by Cloutis & Gaffey (1991) from laboratory studies. Most recently, Burbine et al. (2009) used two values to convert BI minima to BI centre for those asteroids without a visible spectrum: +0.0 or 0.01, depending if the asteroid lies inside the trend defined by the HED or not. This is a strong assumption, because it requires that all V-type asteroids are represented in the HED suite and the fact that some V-type asteroids do not fit the HED band parameters distribution must be due to errors in the band centre evaluation and not due to real compositional differences. If we perform the same kind of correction on our data, the observed spread strongly reduced.

6.2 Correlation of band parameters with orbital parameters

We have also investigated the distribution of orbital elements (proper elements) of the observed asteroids with respect to the band parameters searching for trends and correlations. However, we did not find any clear trend of the band minima with semimajor axis, eccentricity and inclination. Regarding the diameter, no clear trend with BI minima is found, while it seems that BII minima decrease with increasing diameters, as shown in Figs 9(a) and (b).

6.3 Differences between Vesta family and non-Vesta family asteroids

Concerning the differences between (4) Vesta, Vesta family members and non-family members it is difficult to draw a clear

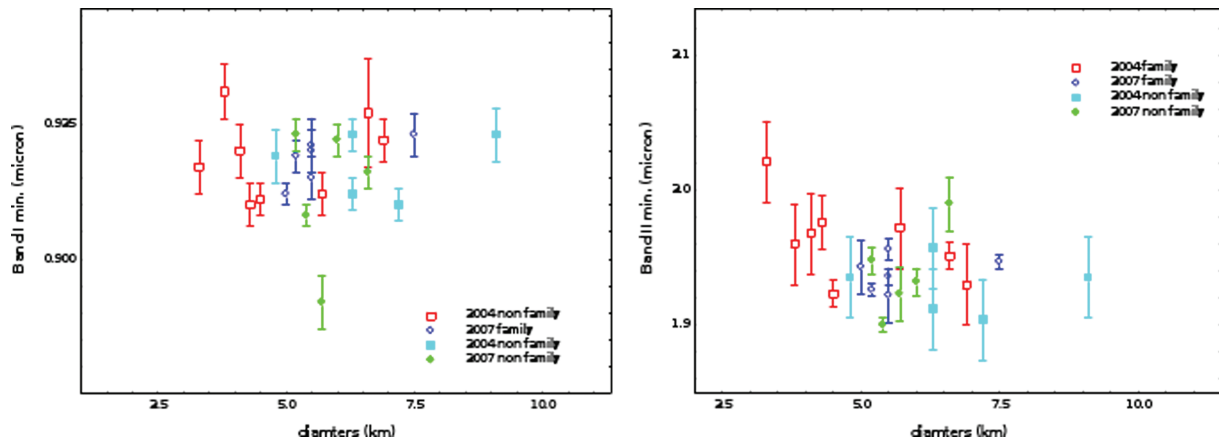


Figure 9. (a) BI minima versus asteroids diameters as reported in Table 1; (b) BII minima versus asteroids diameters as reported in Table 1. Open and filled symbols represent asteroids that are members and non-members of the Vesta dynamical family, respectively.

conclusion. We have analysed the data of 25 asteroids, 15 of them belonging to the Vesta family. In Fig. 8 BI versus BII values of Vesta, HEDs and Vestoids are reported. According to the Gaffey (1997) data, the range of BI and BII centres of Vesta is relatively small, with all spectra falling between the eucrite and diogenite in the BI/BII diagram. Vernazza et al. (2005), instead, reported that BI and BII fall in the transition region between low- and high-calcium pyroxenes close to the diogenites.

With respect to Vesta, the observed asteroids occupy the region with slightly smaller values of BI centre, but not far from the values derived by Vernazza et al. (2005) for Vesta. Several of them overlap the diogenite and howardite regions. The non-family members seem to be more consistent with the HED distribution plot and some of them lie clearly in the diogenitic area. The family members show a large dispersion and seem less consistent with the HEDs values. However, this discrepancy could be due to the larger errors reported for some of the family members.

The inferred [Wo] and [Fs] content of four non-family asteroids is fully consistent with diogenites, while the other non-family members are more similar to howardites (Fig. 7a and b). Only one family member (10349) has content similar to diogenites (Fig. 7a and b); most of them are similar to howardites. It is difficult to say if there is a real prevalence of diogenitic mineralogies among the non-family member or if this is only a statistical fluke, due to the small number of asteroids.

It seems that the [Wo] content of most (14) of the Vesta family members is indicative of howardite mineralogy, while only about half of the non-family member has howardite mineralogy. However, howardite-like asteroids can be objects where both eucrite and diogenite are present or can be asteroids composed of howardite.

The intermediate belt object (21238) 1995WV7 seems to have a spectrum quite different from the spectra of the inner belt V-type asteroids, though its band parameters are similar to those of other few main belt V-type asteroids. As already mentioned, asteroid (21238) 1995WV7 is located beyond the 3:1 resonance, at 2.54 au, and it is unlikely to be related to Vesta as the ejection velocity required is $\sim 1.8 \text{ km s}^{-1}$. The band centres clearly indicate a diogenitic composition for this asteroid, as well as its inferred molar content. Moreover, the very large band depths and areas and the overall spectral slope suggest a quite fresh material on the asteroid surface. According to Moskovitz et al. (2010), in BI versus BII plot, (21238) 1995WV7 is clearly in the region occupied by the diogenites. From a spectral point of view, this object could be a basaltic

asteroids not related with Vesta, thus giving credence to the dynamical arguments. However, this object occupies a region of BI versus BII plot where also some other asteroids, namely (2851) Harbin, (956) Elisa, (8693) Matsuki and (10349) 1992 LN, are present. All these objects overlap only with diogenites in [Fs] and [Wo] plot. Only one of them (10349) is a member of the Vesta family.

7 CONCLUSION

We have observed 12 V-type asteroids measuring their reflectance spectra from 0.7 up to 2.5 μm . We have analysed the new spectra together with those of objects already published, getting a data set of 25 V-type asteroids. A comparison of their band parameters to those of HED meteorites from the RELAB data base reveals a correlation between band centres of the two samples. Using the new methodology in the band analysis, we do not find the wide range of band centres that were reported by Duffard et al. (2004) and the band separation plot constrains very well the revised results. Most of the analysed asteroids show low levels of Ca content (< 10 per cent Wo).

The surface of Vesta is not uniform, showing some dark and bright areas and spectral diversity (Binzel et al. 1997). Its diverse surface makes Vesta one of the most geologically peculiar large asteroids. It is the only asteroid with both albedo and spectral variations across its surface. Gaffey (1997) observed subhemispheric colour and spectral variations across the surface of Vesta, interpreting these differences as regions with differing mineralogies (eucrite- or diogenite-rich surface units). Binzel et al. (1997), with *HST*, observed contrasts in albedo and composition between the Western and Eastern hemispheres suggesting a mainly eucritic mineralogy, for the Western hemisphere, and diogenitic for the east hemisphere. According to Vernazza et al. (2005), the NIR spectra of Vesta show a surface composition closer to diogenites than eucrites and possibly a lower olivine content than those obtained by Gaffey (1997).

The V asteroids here studied have a large range of mineralogy but we see a prevalence of asteroids similar to diogenites and howardite. This result goes in the same direction of Vernazza et al. (2005), suggesting that the spectral diversity observed in the Vestoids arises because these asteroids contain material present on the Vesta surface or coming from different layers of Vesta excavated by collisions and not because they originated from different parent bodies. Nevertheless, from our analysis it seems that there could be an excess of diogenitic mineralogies among the non-family members. However,

the analysed asteroid sample is small to draw clear conclusions and both hypotheses (different parent bodies or common origin) are still valid.

According to our results, if the family members are mainly howardite-like, we must see a predominance of this mineralogy on Vesta's surface. Howardite-like spectra can be characteristics of asteroids where both eucrite and diogenite are present or of asteroids composed of howardite. The latter situation would require a large and thick consolidated regolith on Vesta surface. If also the non-family members are fragments from Vesta, as suggest by some dynamical studies (Carruba et al. 2005), the large spread in band parameters (linked with possibly different pyroxenes mineralogy) seen in the V-type asteroids spectra should be also seen on the Vesta's surface.

The VIR-MS onboard the *Dawn* spacecraft (Russell et al. 2004, De Sanctis et al. 2010) will help to provide insight into Vesta's composition by measuring the spectral reflectance at higher spatial resolution than previous measurements. With a resolution of hundreds of metres per pixel, *Dawn*'s VIR will improve our knowledge of the spectral variability on the surface of Vesta, and therefore allow the distributions of units to be investigated. Those measurements will provide information on the mineralogical regions on the Vesta's surface identified by specific spectra. The spectra spatially resolved of the Vesta's surface acquired by *Dawn* will be compared with those of V-type asteroids and HEDs.

The full disc spectrum of Vesta apparently does not fully match the V-type spectra, the latter being redder and with deeper 1 and 2 μm bands. This difference could arise from the fact that the Vesta spectrum could be an average of different spectral units. In this case, we should expect that the spectra of the single mineralogical unit on Vesta surface would be more similar to the V-type asteroids spectra. The V-family members reflect lithologies that were once present both on the surface of Vesta and possibly also at depth. In particular, it should be possible that at Vesta, VIR on *Dawn* will see the entire range of the V-type asteroids spectra obtained with on ground observations, as well as the range of spectra that we see in the HED meteorites. Future comparisons between band parameters of different regions on Vesta's surface with V-type asteroids may suggest the location from which different Vestoids have been ejected.

The spectral variability on the Vesta's surface that could be measured by VIR will be an important improvement in the process to create a comprehensive picture of the basaltic-rich objects in the asteroid belt.

ACKNOWLEDGMENTS

This work has been supported by an ASI grant, whose support is gratefully acknowledged.

REFERENCES

- Adams J. B., 1974, *J. Geophys. Res.*, 79, 4829
 Adams J. B., 1975, in Karr C., Jr, ed. *Infrared and Raman Spectroscopy of Lunar and Terrestrial Minerals*. Academic Press, San Diego, p. 91
 Alvarez-Candal A., Duffard R., Lazzaro D., Michtchenko T., 2006, *A&A*, 459, 969
 Arai, T., Tomiyama, T., Sakai, K., Takeda H., 2008, 38th Lunar and Planetary Science Conference, 2465
 Beck A. W., McSween H. Y., Jr., 2010, *Meteorit. Planet. Sci.*, 45, 850
 Berkley J. L., Boynton N. J., 1992, *Meteoritics*, 27, 387
 Binzel R. P., Gaffey M. J., Thomas P. C., Zellner B. H., Storrs A. D., Wells E. N., 1997, *Icarus*, 128, 95

- Binzel R. P., Masi G., Foglia S., 2006, Annual Meeting of the Division for Planetary Sciences of the American Astronomical Society, 71.06
 Bunch T. E., Rajan R. S., 1988, *Meteorite Regolithic Breccias*. In: *Meteorites and the Early Solar System (A89-27476 10-91)*. Univ. Arizona Press, Tucson, AZ, p. 144
 Burbine T. H., Buchanan P. C., Binzel R. P., Bus S. J., Hiroi T., Hinrichs J. L., Meibom A., McCoy T. J., 2001, *Meteorit. Planet. Sci.*, 36, 761
 Burbine T. H., Buchanan P. C., Binzel R. P., 2007, 38th Lunar and Planetary Science Conference, 1338, 2117
 Burbine T. H., Buchanan P. C., Dolkar T., Binzel P., 2009, *Meteorit. Planet. Sci.*, 44, 1331
 Burns R. G., 1993, *Mineralogical Applications of Crystal Field Theory*. Cambridge Univ. Press, Cambridge
 Carruba V., Michtchenko T. A., Roig F., Ferraz-Mello S., Nesvorný D. 2005, *A&A*, 441, 819
 Cloutis E. A., 1985. MSc thesis, Univ. Hawaii, Honolulu
 Cloutis E. A., Gaffey M. J., 1991, *J. Geophys. Res.*, 96, 22809
 Cloutis E. A., Gaffey M. J., Jackowski T., Reed K. J., 1986, *J. Geophys. Res.*, 91, 11641
 Cloutis E. A., Gaffey M. J., Smith D. G. W., Lambert R. J., 1990, *J. Geophys. Res.*, 95, 8323
 Delaney J. S., Prinz M., Takeda H., 1984, *J. Geophys. Res.*, 89, Suppl., C251
 De Sanctis M. C. et al., 2010, preprint (doi:10.1007/s11214-010-9668-5)
 Duffard R., Lazzaro D., Licandro J., De Sanctis M. C., Capria M. T., Carvano J. M., 2004, *Icarus*, 171, 120
 Duffard R., Lazzaro D., de León J., 2005, *Meteorit. Planet. Sci.*, 40, 445
 Florczak M., Lazzaro D., Duffard R., 2002, *Icarus*, 159, 178
 Floss C., Taylor L. A., Promprated P., Rumble D., III, 2005, *Meteorit. Planet. Sci.*, 40, 343
 Fowler G. W., Papike J. J., Spilde M. N., Shearer C. K., 1994, *Geochim. Cosmochim. Acta*, 58, 3921
 Gaffey M. J., 1976, *J. Geophys. Res.*, 81, 905
 Gaffey M. J., 1997, *Icarus*, 127, 130
 Gaffey M. J., Bell J. F., Brown R. H., Burbine T. H., Piatek J. L., Reed K. L., Chaky D. A., 1993, *Icarus*, 106, 573
 Gaffey M. J., Cloutis E. A., Kelley M. S., Reed K. L., 2002, in Bottke W. F., Jr, Cellino, A., Paolicchi, P., Binzel, R. P., eds, *Asteroid III*. Univ. Arizona Press, Tucson, p. 183
 Greenwood R. C., Franchi I. A., Jambom A., Buchanan P., 2005, *Nat*, 435, 916
 Hammergren M., Gyuk G., Puckett A. W., 2006, preprint (astro-ph/0609420)
 Hiroi T., Pieters C. M., Takeda H., 1994, *Meteoritics*, 29, 232
 Hiroi T., Binzel R. P., Sunshine J., Pieters C. M., Takeda H., 1995, *Icarus*, 115, 374
 King T. V. V., Ridley I. W., 1987, *J. Geophys. Res.*, 92, 11457
 Klima R. L., Pieters C. M., Dyar M. D., 2008, *Meteorit. Planet. Sci.*, 42, 235
 Larson H. P., Fink U., 1975, *Icarus*, 26, 420
 Lazzarin M., Marchi S., Barucci M. A., Di Martino M., Barbieri C., 2004, *Icarus*, 169, 373
 Lazzaro D. et al., 2000, *Sci*, 288, 2033
 Licandro J., Ghinassi F., Testi L., 2002, *A&A*, 388, L9
 Lindstrom M. M., Mittlefehldt D. W., 1992, *Meteoritics*, 27, 250
 Marchi S., De Sanctis M. C., Lazzarin M., Magrin S., 2010, *ApJ*, 721, L172
 Marzari F., Cellino A., Davis D. R., Farinella P., Zappalá V., Vanzani V., 1996, *A&A*, 316, 248
 Mayne R. G., Sunshine J. M., Bus S. J., McCoy T. J., McSween H. Y., Gale A., Corrigan C. M., 2007, 38th Lunar and Planetary Science Conference, 1338, 1157
 McCord T. B., Adams J. B., Johnson T. V., 1970, *Sci*, 168, 1445
 McFadden L. A., McCord T. B., Pieters C., 1977, *Icarus*, 31, 439
 McSween H. Y., Mittlefehldt D. W., Beck A. W., Mayne R. G., McCoy T. J., 2010, *Space Science Reviews*, Online First, doi:10.1007/s11214-010-9637-z
 Mittlefehldt D. W., 1994, *Geochim. Cosmochim. Acta*, 58, 1537

- Mittlefehldt D. W., McCoy T. J., Goodrich C. A., Kracher A., 1998, in Papike J. J., ed., *Reviews in Mineralogy*, Vol. 36, Planetary Materials. Mineralogical Society of America, Washington, p. 4
- Moskovitz N. A., Jedicke R., Gaidos E., Willman M., Nesvorný D., Fevig R., Izevic Z., 2008, *Icarus*, 198, 77
- Moskovitz N., Willman M., Burbine T., Binzel R., Bus S., 2010, preprint, 208, 773
- Mothé-Diniz T., Roig F., Carvano J. M., 2005, *Icarus*, 174, 54
- Pieters C. M., Hiroi T., 2004, *LPSC*, 1720
- Russell C. T. et al., 2004, *PSS*, 52, 465
- Russell C. T. et al., 2007, *Adv. Space Res.*, 40, 193
- Sack R. O., Azeredo W. J., Lipschutz M. E., 1991, *Geochim. Cosmochim. Acta*, 55, 1111
- Scott E. R. D., Greenwood R. C., Franchi I. A., Sanders I. S., 2009, *Geochim. Cosmochim. Acta*, 73, 5835
- Shestopalov D. I., McFadden L. A., Golubeva L. F., Orujova L. O., 2010, *Icarus*, doi:10.1016/j.icarus.2010.04.012
- Sunshine J. M., Pieters C. M., 1993, *J. Geophys. Res.*, 98, NO. E5, 9075
- Takeda H., 1997, *Meteorit. Planet. Sci.*, 32, 841
- Takeda H., Graham A. L., 1991, *Meteoritics*, 26, 129
- Tedesco E. F., 1989, in Binzel R. P., Gehrels T., Matthews M. S., eds, *Asteroids II*, Univ. Arizona Press, Tucson, p. 1090
- Vernazza P., Mothé-Diniz T., Barucci M. A., Birlan M., Carvano J. M., Strazzulla G., Fulchignoni M., Migliorini A., 2005, *A&A*, 436, 1113
- Vilas F., Cochran A. L., Jarvis K. S., 2000, *Icarus*, 147, 119
- Xu S., Binzel R. P., Burbine T. H., Bus S. J., 1995, *Icarus*, 115, 1
- Yamaguchi A. et al., 2002, *Sci*, 296, 334

This paper has been typeset from a MS Word file prepared by the author.